HHS Public Access

Author manuscript

Nature. Author manuscript; available in PMC 2013 September 17.

Published in final edited form as:

Nature. ; 475(7356): 377–380. doi:10.1038/nature10194.

Amygdala to nucleus accumbens excitatory transmission facilitates reward seeking

Garret D. Stuber[1,2,*], **Dennis R. Sparta**[1,2], **Alice M. Stamatakis**[1], **Wieke A. van Leeuwen**[2], **Juanita E. Hardjoprajitno**[2], **Saemi Cho**[2], **Kay M. Tye**[2], **Kimberly A. Kempadoo**[2], **Feng Zhang**[3], **Karl Deisseroth**[3], and **Antonello Bonci**[2,4]

[1]Departments of Psychiatry & Cell and Molecular Physiology, UNC Neuroscience Center, University of North Carolina at Chapel Hill, Chapel Hill, NC USA

[2]Ernest Gallo Clinic and Research Center, Department of Neurology, Wheeler Center for the Neurobiology of Drug Addiction, University of California San Francisco, San Francisco, CA USA

[3]Departments of Bioengineering & Psychiatry and Behavioral Sciences, Stanford University, Stanford, CA USA

[4]Intramural Research Program, National Institute on Drug Abuse, Baltimore, MD USA

Abstract

The basolateral amygdala (BLA) plays a crucial role in emotional learning irrespective of valence[1–5]. While the BLA projection to the nucleus accumbens (NAc) is hypothesized to modulate cue-triggered motivated behaviors[4, 6, 7], our understanding of the interaction between these two brain regions has been limited by the inability to manipulate neural circuit elements of this pathway selectively during behavior. To circumvent this limitation, we used *in vivo* optogenetic stimulation or inhibition of glutamatergic fibers from the BLA to the NAc, coupled with intracranial pharmacology and *ex vivo* electrophysiology. We show that optical stimulation of the BLA-to-NAc pathway in mice reinforces behavioral responding to earn additional optical stimulations of these synaptic inputs. Optical stimulation of BLA-to-NAc glutamatergic fibers required intra-NAc dopamine D1-type, but not D2-type, receptor signaling. Brief optical inhibition of BLA-to-NAc fibers reduced cue-evoked intake of sucrose, demonstrating an important role of this specific pathway in controlling naturally occurring reward-related behavior. Moreover, while optical stimulation of medial prefrontal cortex (mPFC) to NAc glutamatergic fibers also elicited reliable excitatory synaptic responses, optical self-stimulation behavior was not observed by activation of this pathway. These data suggest that while the BLA is important for processing both positive and negative affect, the BLA-to-NAc glutamatergic pathway in conjunction with dopamine signaling in the NAc promotes motivated behavioral responding.

[*]Address correspondence to: Garret D. Stuber, Ph.D., Assistant Professor, Departments of Psychiatry & Cell and Molecular Physiology, UNC Neuroscience Center, University of North Carolina at Chapel Hill, Tel: +1 (919) 843-7140, Fax: +1 (919) 966-1050, gstuber@med.unc.edu.

Author Contributions:

G.D.S. and A.B. designed, discussed, and planned all experiments. G.D.S., D.R.S., A.M.S., W.L., J.H. S.C., K.M.T. and K.K. performed experiments. G.D.S., D.R.S., A.M.S., and W.L. analyzed data. F.Z. and K.D. provided resources and training to G.D.S. G.D.S. and A.B. wrote the manuscript.

To stimulate excitatory fibers projecting from the BLA to the NAc selectively, we stereotaxically delivered adeno-associated viral vectors carrying the codon-optimized channelrhodopsin-2 gene in-frame fused to enhanced yellow fluorescent protein (ChR2-EYFP)[8] driven by the CaMKIIα promoter to transduce glutamatergic neurons locally in the BLA. Expression of ChR2-EYFP was observed following transduction of neurons in the BLA (Fig. 1a). Whole-cell recordings from visually-identified BLA pyramidal neurons expressing ChR2 revealed that light stimulation frequencies (1 – 20 Hz, 5ms light pulses) resulted in reliable firing in response to light with minimal loss of spike fidelity at 20 Hz (Fig. 1b, Supplementary Fig. 1), indicating optically-induced firing via activation of ChR2 is capable of exciting BLA neurons at physiologically-relevant frequencies[5, 6]. Expression of ChR2-EYFP was observed in forebrain targets of the BLA, including the NAc (Fig. 1c). Optical stimulation of ChR2-EYFP-positive fibers and synaptic terminals from the BLA-to-NAc resulted in excitatory responses in the NAc (Fig. 1d, Supplementary Fig. 2). Light-evoked excitatory postsynaptic currents (EPSCs) from visually identified medium spiny neurons were blocked by bath application of 10 μM of the competitive α-amino-3-hydroxy-5-methyl-4-isoxazolepropionic acid receptor (AMPAR) antagonist 6-cyano-7-nitroquinoxaline-2,3-dione (CNQX), demonstrating that optical stimulation of BLA-to-NAc fibers results in AMPAR-mediated EPSCs via the release of synaptic glutamate (Fig. 1f).

To test whether selective activation of BLA-to-NAc synapses could promote motivated behavioral responding, mice injected with ChR2-EYFP or EYFP control virus into the BLA were stereotactically implanted with a guide cannula above the ipsilateral NAc. 21 – 28 d post-surgery, a fiber-optic cable connected to a laser capable of activating ChR2 was positioned directly above the NAc for optical stimulation (Supplementary Fig. 3). Mice were then placed in behavioral testing chambers equipped with two ports: an active port, which when triggered by beam breaks from nosepoke responses, produced an optical stimulation train to activate BLA-to-NAc fibers selectively, and an inactive port that produced no optical stimulation. Mice expressing ChR2-EYFP in BLA-to-NAc terminals readily learned to perform nosepoke responses to earn optical stimulations, in contrast to EYFP-expressing controls, in a single 60-min behavioral session (Fig. 2a,b, Supplementary movie 1, Supplementary Fig. 4). Inactive nosepoke responses were not significantly different between ChR2-EYFP and EYFP controls, implying that optical stimulation of BLA-to-NAc fibers did not cause an increase in general responding (Fig. 2b). In contrast, direct optical activation of BLA cell bodies was highly variable in promoting self-stimulation behavior (Supplementary Fig. 5).

To determine whether optical stimulations of BLA-to-NAc fibers reinforced nosepoke behavior and thus increased the likelihood of additional behavioral responses, laser stimulations were withheld while active nosepoke responses were recorded in a behavioral session. ChR2-EYFP-expressing mice showed a significant decrease in responding when optical stimulations were withheld for 1 hr (Supplementary Fig. 6). In addition, mice demonstrated a rapid renewal of self-stimulation behavior when optical stimuli were delivered non-contingently and subsequent nosepoke responses were again reinforced following the 1-hr extinction period.

Many forms of motivated behaviors depend on dopaminergic[9, 10, 11] as well as glutamatergic signaling within the NAc[6, 7, 12]. To test whether optical self-stimulation behavior of BLA-to-NAc fibers was dependent on DAergic signaling, mice trained previously in the optical self-stimulation task were administered microinjections into the NAc (through the same guide cannula used to introduce the optical fiber) with either vehicle, a D1R antagonist, (SCH23390) or a D2R antagonist (raclopride) immediately before optical self-stimulation sessions. D2R antagonism (tested at two doses, Supplementary Fig. 7) had no effect, while D1R antagonism significantly decreased the number of active nosepokes (Fig. 2c,d). Additionally, D1R antagonism did not reduce the rate of responding in the beginning of the behavioral session, nor did it affect the rate of responding within a burst of nosepokes, suggesting decreased responding during the entire session was not due to locomotor impairments induced by unilateral D1R antagonism (Supplementary Fig. 8). Importantly, application of SCH23390 to NAc brain slices expressing ChR2 in BLA-to-NAc fibers significantly decreased the amplitude of all EPSCs evoked by the same optical stimulation train (60p at 20 Hz) that reinforced nosepoking behavior (Supplementary Fig. 9). These data suggest that the reinforcing properties of BLA-to-NAc stimulation require glutamate release from BLA terminals, which has postsynaptic effects on MSNs that are modulated by D1Rs.

Activation of BLA-to-NAc fibers may produce action potentials that back-propagate to cell bodies in the BLA, which could then activate axon collaterals that project to other brains regions. Therefore, in mice trained previously to self-stimulate, we tested whether BLA-to-NAc optical self-stimulation required neural activity in the BLA by inactivating it with intracranial injections of lidocaine immediately prior to self-stimulation sessions. Ipsilateral BLA inactivation had no effect on acquisition (Supplementary Fig. 10) or expression optical self-stimulation behavior (Fig. 2e,f), demonstrating that the reinforcing properties of the optical stimulation were mediated by BLA glutamatergic fibers in the NAc or fiber collaterals outside of the BLA.

To determine whether activity of BLA-to-NAc fibers was required for naturally occurring motivational processing, we performed pathway-specific optical inactivation experiments in a separate behavioral task where mice were trained to drink a sucrose solution in response to a reward-predictive cue. The BLA was bilaterally injected with a virus coding for the light-gated Cl^- pump, NpHR[13] (AAV-CaMKIIα-NpHR3.0-EYFP; Supplementary Fig. 11). Whole cell recordings from brain slices containing NpHR-expressing BLA neurons revealed that 500 ms pulses of 532 nm light delivered to the slice resulted in prominent outward currents (146.2 ± 61.4 pA; n = 5 cells) when neurons were voltage-clamped at −60 mV. Current injections that reliably produced trains of action potentials were inefficient at eliciting spiking when NpHR was activated (Fig. 3a). In a subset of mice, where BLA neurons were transduced with virus to express both ChR2 and NpHR, stimulation of BLA-to-NAc terminals via activation of ChR2 with 473 nm light resulted in light-evoked EPSCs as predicted. However, when NpHR was simultaneously active in BLA-to-NAc fibers, ChR2 activation resulted in significantly more failed EPSCs (Fig. 3b). Thus, NpHR activation was capable of reducing evoked BLA-to-NAc EPSCs, and therefore should also reduce endogenous activity of BLA-to-NAc fibers *in vivo*.

Mice with optical fibers implanted above the NAc and expressing NpHR in BLA-to-NAc fibers underwent four conditioning sessions consisting of 50 trials where a 5 s tone/houselight stimulus predicted the delivery of 20 μl of 20% sucrose. Motivated behavioral responding was assayed by the number of licks each mouse made at the sucrose receptical. On each cue-reward pairing, BLA-to-NAc fibers were transiently inactivated by bilaterally delivering laser pulses 200 ms prior to cue onset and terminating 200 ms after cue offset (laser on for 5.4 s per trial, Supplementary Fig. 12). Laser illumination was delivered in an identical fashion to control mice only expressing EYFP. Over the four conditioning sessions, EYFP control mice developed robust time-locked licking behavior in response to the reward-predictive stimulus as well as to subsequent sucrose delivery (Fig. 3c–e). In contrast, mice that received transient inhibition of BLA-to-NAc fibers during the cue-reward pairing period showed a significant attenuation of licking in response to the cue or to subsequent reward delivery (Fig. 3c–e). Transient BLA-to-NAc inactivation during cue-reward pairing also reduced the total number of licks throughout the entire session. However, when NpHR-expressing mice underwent an additional sucrose responding session, but without laser inhibition of the BLA-to-NAc fibers, total session licking returned to levels similar to those observed in EYFP control mice, demonstrating that the presence of NpHR alone (without optical modulation) was not sufficient to alter licking behavior (Supplementary Fig. 13). These data demonstrate that brief, transient inhibition of BLA-to-NAc fibers can reduce motivated behavioral responding to obtain natural rewards.

In addition to the glutamatergic projection from the BLA, the NAc receives excitatory synaptic inputs from infralimbic and prelimbic regions of the mPFC[14] that are thought to modulate compulsive reward-seeking[15, 16]. To determine whether activation of mPFC-to-NAc excitatory synaptic connections promote reward-seeking behavior similar to BLA-to-NAc activation, additional mice were injected with ChR2-EYFP virus into the mPFC (Fig. 4a), which resulted in expression of ChR2-EYFP in fibers and synaptic terminals in the NAc (Fig. 4b). Mice were then tested to determine whether optical activation of mPFC-to-NAc fibers (Supplementary Fig. 14) supported self-stimulation behavior similar to BLA-to-NAc activation. Notably, mice expressing ChR2-EYFP at mPFC-to-NAc showed no difference in active or inactive nosepokes made relative to EYFP-expressing control mice (Fig. 4c). ChR2-EYFP expressing mPFC neurons were optically excitable (Supplementary Fig. 15), and optically-evoked mPFC-to-NAc were readably detectable (Supplementary Fig. 16), demonstrating that optical activation of the mPFC-to-NAc inputs induced glutamate release, but did not support optical self-stimulation.

To determine whether quantitative differences existed in the amount of glutamate released from these two pathways, fluorescence-guided, whole-cell recordings in the NAc were performed while varying the light-stimulus intensity in separate groups of mice selectively expressing ChR2 in either the BLA or mPFC-to-NAc pathway. In NAc neurons that showed clear light evoked EPSCs, BLA-to-NAc evoked EPSCs were approximately twice the amplitude of those evoked following mPFC-to-NAc stimulation at maximal light intensities (Fig. 4d). In addition, NAc neurons typically showed excitatory postsynaptic responses to both optical stimulation of BLA inputs and electrical stimulation of cortical afferents (Supplementary Fig. 17), suggesting that NAc MSNs receive both mPFC and BLA inputs, but that mPFC inputs release less glutamate.

These results also show that selective activation of BLA but not mPFC glutamatergic inputs to the NAc promote motivated behavioral responding, consistent with the hypothesized role of BLA inputs in facilitating responding to cues and mPFC inputs in suppressing inappropriate actions[16]. DA signaling capable of activating D1Rs during optical self-stimulation sessions could arise from the burst firing of DAergic neurons time-locked to salient stimuli during behavioral responding[17, 18]. Alternatively, glutamate released from BLA terminals may directly gate the release of DA from DAergic fibers in the NAc independent of VTA neuronal activity[19, 20]. In conclusion, our results demonstrate that afferent-specific glutamatergic neurotransmission from the BLA to the NAc is both necessary and sufficient to promote the expression of motivated behavioral responding.

Methods Summary

Opsin delivery to neural tissue

AAV-CaMKIIα-ChR2-EYFP, AAV-CaMKIIα-EYFP, and AAV-CaMKIIα-NpHR3.0-EYFP packaged as AAV5 by the UNC Vector Core Facility. Virus (0.5 μl) was stereotactically injected into the BLA or mPFC at a rate 0.1 μl/min via 26 gauge injector needles coupled to a 2 μl Hamilton syringe. Mice were used for experiments ~28 d after virus injections.

Brain slice electrophysiology

Opsin expressing mice were deeply anesthetized, decapitated, and 200 μm sections of the BLA, NAc, or mPFC were prepared. Whole cell voltage clamp recordings were performed using a Cesium methylsulfonate and current clamp recordings were performed using a potassium gluconate internal solution. 1 – 5 ms of 473, 532, or 593.5 nm light was delivered via a fiber-coupled laser.

In vivo optogenetic stimulation and inhibition during behavior

Mice injected with opsin coding viral constructs were implanted with guide cannula or chronic optical fibers directly above the NAc. Acute or chronic optical implants were connected to optical patch cables coupled to 473 or 532 nm lasers that were modulated by a stimulus pulse generator. Laser pulse onset was controlled by signal pulses generated by behavioral hardware (Med Associates).

Online materials and methods

Experimental subjects and stereotaxic surgery

Adult (25–30g) male C57BL/6J mice (Jackson Laboratory, Bar Harbor, ME) were group-housed until surgery. Mice were maintained on a 12:12 light cycle (lights on at 07:00). Once the animals were acclimated to the animal facility for ~1 week, they were anesthetized with 150 mg/kg ketamine 50 mg/kg xylazine and placed in a stereotaxic frame (Kopf Instruments). Microinjection needles were then inserted bilaterally directly above the BLA (coordinates from Bregma: −1.6 AP, ±3.1 ML, −4.9 DV). Microinjections were performed using custom-made injection needles (26 gauge) connected to a 2 μl Hamilton syringe. Each BLA was injected with 0.3 – 0.5 μl of purified and concentrated AAV (~10^{12} infectious

units/mL) coding ChR2-EYFP, NpHR3.0-EYFP, or EYFP under control of the CaMKIIα promoter over 10 minutes followed by an additional 10 minutes to allow diffusion of viral particles away from the injection site. For optical self-stimulation experiments mice were first injected unilaterally in the BLA with virus and then a guide cannula was implanted directly over the ipsilateral NAc (+1.3 AP, ±1.0 ML, −4.0 DV) to allow for insertion of the fiber optic cable during the experiment, which was secured to the skull using Geristore (www.denmat.com) dental cement. Mice were then returned to their home cage. Body weight and signs of illness were monitored until recovery from surgery (approx. 2 weeks). All procedures were conducted in accordance with the Guide for the Care and Use of Laboratory Animals, as adopted by NIH, and with approval of the UNC and UCSF Institutional Animal Care and Use Committees.

Construct and AAV preparation

DNA plasmids coding pAAV-CaMKIIα-ChR2-EYFP (H134R), pAAV-CaMKIIα-NpHR3.0-EYFP, or pAAV-CaMKIIα-EYFP were obtained from the laboratory of Karl Deisseroth (see www.optogenetics.org for additional details). Plasmid DNA was amplified, purified, and collected using a standard plasmid maxiprep kit (Qiagen). Following plasmid purification, restriction digest, and sequencing to assure DNA fidelity, purified recombinant AAV vectors were serotyped with AAV5 coat proteins and packaged using calcium phosphate precipitation methods by the UNC Vector Core facilities (University of North Carolina, Chapel Hill). The final viral concentration was 1–2 × 10^{12} genome copies/mL.

Slice preparation for patch-clamp electrophysiology

Mice were anesthetized with pentobarbital and perfused transcardially with modified aCSF containing (in mM): 225 sucrose, 119 NaCl, 2.5 KCl, 1.0 NaH_2PO_4, 4.9 $MgCl_2$, 0.1 $CaCl_2$, 26.2 $NaHCO_3$, 1.25 glucose. The brain was removed rapidly from the skull and placed in the same solution used for perfusion at ~0°C. Coronal sections of the NAc or BLA (200 μm) were then cut on a vibratome (VT-1200, Leica Microsysytems). Slices were then placed in a holding chamber and allowed to recover for at least 30 min before being placed in the recording chamber and superfused with bicarbonate-buffered solution saturated with 95% O2 and 5% CO_2 and containing (in mM): 119 NaCl, 2.5 KCl, 1.0 NaH_2PO_4, 1.3 $MgCl_2$, 2.5 $CaCl_2$, 26.2 $NaHCO_3$, and 11 glucose (at ~32°C).

Patch-clamp electrophysiology

Cells were visualized using infrared differential interference contrast and fluoresce microscopy. Whole-cell voltage-clamp or current clamp recordings of BLA and NAc neurons were made using an Axopatch 200A or B amplifier. Patch electrodes (3.0 – 5.0 MΩ) were backfilled with internal solution containing 130 mM KOH, 105 mM methanesulfonic acid, 17 mM hydrochloric acid, 20 mM HEPES, 0.2 mM EGTA, 2.8 mM NaCl, 2.5 mg/ml MgATP, and 0.25 mg/ml GTP (pH 7.35, 270–285 mOsm). Series resistance (15 – 25 MΩ) and/or input resistance were monitored online with a 4 mV hyperpolarizing step (50 ms) given between stimulation sweeps. All data was filtered at 2 kHz, digitized, and collected using pClamp10 software (Molecular Devices). For current clamp experiments to characterize cell firing, 10 pulses at frequencies of 1, 5, 10, and 20 Hz, respectively, were tested to determine spike fidelity (the percentage of light pulses that lead

to action potentials). For optical stimulation of EPSCs, stimulation (pulses of 1 – 2 mW, 473 nm light delivery via a 200 μm optical-fiber coupled to a solid-state laser) was used to evoke presynaptic glutamate release from BLA projections to the NAc. NAc MSNs were voltage-clamped at −70 mV. For pharmacological characterization of glutamate currents, light-evoked EPSCs were recorded for 10 min followed by bath application of 10 μM CNQX for an additional 10 min. 10–12 sweeps pre- and post-drug were averaged and peak EPSCs amplitudes were then measured. For EPSC pulse train experiments, input-specific currents were evoked by 60 optical pulses (20 Hz stimulation, 5 ms pulse duration.). This was repeated 12 times at 0.1 Hz. 4 μM SCH23390 or vehicle was then bath applied for 10 min and the stimulus train was again repeated. The average EPSC train from the 6 sweeps immediately prior to drug application and those for the 6 sweeps immediately after drug application were then compared.

In vivo optrode recording

Approximately, 21 – 28 d after bilateral AAV-CaMKIIα-ChR2-EYFP injection into the BLA, mice were deeply anesthetized with ketamine/xylazine and placed in a stereotaxic frame equipped with a temperature controller to regulate body temperature. The skull was then removed directly above the NAc. Parylene coated tungsten electrodes (1 MΩ), epoxied to an optical fiber 200 μm core diameter, 0.37 N.A.) coupled to a 473 nm laser were then lowered into the NAc to record unit activity of postsynaptic MSNs following trains of light pulses used to evoke BLA-to-NAc-specific glutamate release. Ten pulses of light (10 – 20 mW, 5 ms) at frequencies of 1, 5, 10, and 20 Hz, respectively, were used to determine spike fidelity *in vivo* analogous to what was with performed during whole-cell recording. Unit activity was amplified with an extracellular amplifier (A-M systems), band-pass filtered at 300Hz low/5 kHz, and digitized using pClamp10 software.

Freely moving optical self-stimulation

21 – 28 d following injection of pAAV-CaMKIIα-ChR2-EYFP or control virus into the BLA, mice with cannula placed above the NAc were prepared for nosepoke training. Mice were mildly food restricted to four grams of food per day to stabilize body weight and facilitate behavioral responding. Body weight was monitored throughout the experiment and did not fall below ~90% of their free feeding weight. Immediately before placing mice in the operant chambers, stylets were removed from the cannula, and a flat cut 125 μm diameter fiber optic cable, coupled to a solid state 473 nm laser outside of the operant chamber, was inserted through the guide cannula and placed directly above the NAc. Immediately prior to insertion, through the guide cannula, light output through the optical fibers was adjusted to 10 – 20 mW. The optical fiber was then secured into place via a custom-made locking mechanism to ensure no movement of the fiber occurred during the experiment. Mice were then placed in standard Med-Associates operant chambers equipped with an active and inactive nosepoke operandum directly below two cue lights. The chambers were also equipped with house lights, audio stimulus generators, and video cameras coupled to DVD recorders. A one hour optical self-stimulation session began with the onset of the cue light above the active nosepoke operandum. Each active nosepoke performed by the animal resulted in an optical stimulation of BLA-to-NAc fibers (60 pulses, 20 Hz, 5 ms pulse

duration). Both active and inactive nosepoke timestamp data was recorded using Med-PC software and analyzed using Neuroexplorer and Microsoft Excel software.

NAc microinjections prior to optical self-stimulation

Stylets were removed from guide cannula and a 26-gauge injector needle connected to a 1 μL Hamilton syringe was inserted. All microinjections were delivered in 0.3 μl sterile saline at a rate of 0.1 μl/min. Injector needles remained in place for an additional 2 min before being removed and replaced immediately with wither stylets or optical fibers for self-stimulation sessions. Doses of drugs used for microinjections were: 600 ng/0.3 μl for SCH23390; 100 ng/0.3 μl and 3 μg/0.3 μl for raclopride, and 10 ug/0.3 μl for lidocaine.

Implantable optical fibers for NpHR inhibition during behavior

For these experiments, mice were bilaterally injected into the BLA with virus coding for NpHR3.0-EYFP or EYFP as described above. Mice were also implanted with bilateral optical fibers targeted directly above each NAc. Optical fibers were constructed in-house by interfacing a 7 – 10 mm piece or 200 μm, 0.37 NA optical fiber with a 1.25 mm zirconia ferrule (fiber extending 5 mm beyond the end of the ferrule.) Fibers were epoxied into ferrules, and cut and polished. After construction, all fibers were calibrated to determine a percentage of light transmission at the fiber tip that would interface with the brain. Prior to bilateral implantation, fibers were matched to each other so that each fiber output equal amounts of light (within 10%). This was done to ensure that an equal amount of light was delivered to each hemisphere. Following surgery, protective plastic caps were placed on the implanted optical fibers to protect them from dust and debris.

Four to five weeks after implantation surgery and three days prior to the experiment, mice were connected to ‘dummy’ optical patch cables each day for 30 – 60 min to habituate them to the tethering procedure in their home cage. On experiment days, protective caps were removed from the implanted fibers. Fibers were then connected to custom-made optical patch cables (62.5 μm core diameter) that were covered with furcation tubing to protect the cables and prevent light from the laser from illuminating the operant chamber. Bilateral fibers were connected to a fiber splitter (50:50 split ratio) that interfaced with a fiber-coupled 532 nm DPSS laser (200 mW). Based on each pair of fibers’ calibration factor, light intensity was set to 10 mW illumination at each fiber tip in the brain.

Optical inhibition of BLA-to-NAc fibers during sucrose responding

Mice with optical fibers implanted above the NAc and expressing either NpHR3.0-EYFP or EYFP in BLA-to-NAc fibers were trained to drink sucrose in response to an environmental stimuli that predicted sucrose delivery. The start of the session was signaled by the onset of white noise in the operant chamber. Each session consisted of 50 cue-reward pairings with a random inter-trial interval of 120 s. During each trial, a TTL was sent from the behavioral hardware to engage the laser 200 ms prior to the onset of a 5 s reward-predictive stimulus (tone/house light compound stimulus). Delivery of 20 μl of 20% sucrose to a receptacle occurred immediately after the termination of the reward-predictive cue, and the laser pulse was terminated 200 ms after cue offset. Starting and extending the laser pulse 200 ms before and after the cue were done based on *in vitro* experiments where we observed that activation

of NpHR led to maximal inhibition 200 ms after the start of the laser pulse. Cue presentation, reward delivery, lick, and laser timestamps were stored as separate data arrays and analyzed offline with Microsoft Excel and Neuroexplorer.

Timelocked licking behavior was quantified for all mice. Mice that did not make at least 200 licks on at least one of the four conditioning sessions were excluded from analysis. This resulted in the removal of n = 2 NpHR and n = 2 EYFP mice from analysis. Timelocked lick histograms with 0.5s time bins were then constructed from −10 – 30 s timelocked to cue onset (t = 0). Lick rates were normalized to baseline periods using a z-score procedure ($z = (x - \mu)/\sigma$) where the μ was the average lick rate and σ was the standard deviation in the 10 s preceding the cue onset.

Data analysis

Statistical significance was assessed using t-tests or analysis of variance (ANOVA) followed by post-hoc tests when applicable using an $\alpha = 0.05$. Data was analyzed using Microsoft Excel with the Statplus plugin and Prism (GraphPad Software).

Virus expression and histology

Following behavioral experiments, mice were deeply anesthetized with pentobarbital and perfused transcardially with phosphate buffered saline (PBS) followed by 4% paraformaldehyde (PFA) dissolved in PBS. Brains were removed carefully and post-fixed in 4% PFA for an additional 24 – 48 hrs. Brains were transferred to 30% sucrose for 48 – 72 hrs before slicing 50 μm sections of the BLA or NAc on a freezing stage microtome or cryostat. Slices were then triple washed in PBS for 5 min. Slices were then stained with 2% Neurotrace fluorescent Nissl stain (Invitrogen; excitation 530 nm, emission 615 nm) diluted in PBS with 0.1% Triton X-100, for 1 hr. Slices were then washed and mounted on gelatin-coated slides, treated with fluorescent-mounting media, and coverslipped. Expression of ChR2-EYFP, NpHR3.0-EYFP, or EYFP was then examined for all mice using either a Nikon inverted fluorescent microscope with a 4, 10, or 20X objective or a Zeiss laser-scanning confocal microscope at 25 and 63X. Following injection of virus into the BLA, robust expression of ChR2-EYFP was observed in BLA projection targets including the NAc, mPFC, hippocampus, insular cortex, and to a lesser extent, the dorsal medial striatum. Mice showing no EYFP expression in the NAc due to faulty microinjections or mice showing cannula or fiber placements outside of the NAc were excluded from analysis.

Reconstruction of optical stimulation or inhibition sites in the NAc

To determine optical stimulation sites in experiments where guide cannulas were used to introduce optical fibers into brain tissue (BLA-to-NAc and mPFC-to-NAc optical self-stimulation experiments, see Supplementary Figs. 3, 14 for location of optical stimulation sites), fixed and stained coronal brain sections (see above) containing the NAc and cannula tracks were examined on an upright conventional fluorescent microscope. Cannula tracks were located in the slices and optical stimulation sites were determined by locating the site 1 mm ventral to the end of the cannula tip. A 1 mm distance was used in these experiments because the optical fibers extended 0.5 mm beyond the end of the cannula (each fiber was cut to this length prior to insertion). Based on light output from these optical fibers (477

mW*mm^{-1} at the tip and calculating intensity taking into account geometric loss and scattering through tissue[1] loss at 0.5 mm beyond the fiber tip led to an estimated 2.6% transmission or 12.4 mW*mm^{-1} at this distance. At 1 mm from the tip of the optical fiber, estimated transmission dropped to 0.56% or 2.67 mW*mm^{-1}, which approximates the minimum intensity required to activate opsin proteins (1 mW*mm^{-1}). For NpHR-mediated inhibition experiments, optical inhibition sites (Supplementary Fig. 11) were determined in a similar fashion; with 0.5 mm used as the distance from fiber tip to the diagrammed inhibition sites, as no guide cannula was present. 0.5 mm beyond the optical fiber tip represents the center location where optical stimulation or inhibition occurs, (0.5 mm above and below). All calculations were performed using equations and constants listed in Aravanis et al., 2007[21].

Supplementary Material

Refer to Web version on PubMed Central for supplementary material.

Acknowledgments

We thank Jana Phillips, Viktor Kharazia, Antoine Adamantidis, and Hsing-Chen Tsai for assistance and advice. We also thank Vladimir Gukassyan and the UNC Neuroscience Center Microscopy Core Facility. This study was supported by funds from NARSAD, ABMRF, The Foundation of Hope, NIDA (DA029325), and startup funds provided by the Psychiatry Department at UNC Chapel Hill (G.D.S.), and from the State of California through the University of California at San Francisco (A.B). D.R.S. was supported by F32AA018610.

References

1. Balleine BW, Killcross S. Parallel incentive processing: an integrated view of amygdala function. Trends in Neurosciences. 2006; 29(5):272–279. [PubMed: 16545468]
2. Maren S, Quirk GJ. Neuronal signalling of fear memory. Nature Rev Neurosci. 2004; 5(11):844–852. [PubMed: 15496862]
3. LeDoux J. The emotional brain, fear, and the amygdala. Cell Mol Neurobiol. 2003; 23(4–5):727–738. [PubMed: 14514027]
4. Cador M, Robbins TW, Everitt BJ. Involvement of the amygdala in stimulus-reward associations: Interaction with the ventral striatum. Neuroscience. 1989; 30(1):77–86. [PubMed: 2664556]
5. Tye KM, Stuber GD, de Ridder B, Bonci A, Janak PH. Rapid strengthening of thalamo-amygdala synapses mediates cue-reward learning. Nature. 2008; 453(7199):1253–1257. [PubMed: 18469802]
6. Ambroggi F, Ishikawa A, Fields HL, Nicola SM. Basolateral amygdala neurons facilitate reward-seeking behavior by exciting nucleus accumbens neurons. Neuron. 2008; 59(4):648–661. [PubMed: 18760700]
7. Di Ciano P, Everitt BJ. Direct interactions between the basolateral amygdala and nucleus accumbens core underlie cocaine-seeking behavior by rats. J Neurosci. 2004; 24(32):7167–7173. [PubMed: 15306650]
8. Zhang F, Wang LP, Boyden ES, Deisseroth K. Channelrhodopsin-2 and optical control of excitable cells. Nature Methods. 2006; 3(10):785–792. [PubMed: 16990810]
9. Phillips PE, Stuber GD, Heien ML, Wightman RM, Carelli RM. Subsecond dopamine release promotes cocaine seeking. Nature. 2003; 422(6932):614–618. [PubMed: 12687000]
10. Stuber GD, Klanker M, de Ridder B, Bowers MS, Joosten RN, Feenstra MG, Bonci A. Reward-predictive cues enhance excitatory synaptic strength onto midbrain dopamine neurons. Science. 2008; 321(5896):1690–1692. [PubMed: 18802002]
11. Tsai HC, Zhang F, Adamantidis A, Stuber GD, Bonci A, de Lecea L, Deisseroth K. Phasic firing in dopaminergic neurons is sufficient for behavioral conditioning. Science. 2009; 324(5930):1080–1084. [PubMed: 19389999]

12. Di Ciano P, Cardinal RN, Cowell RA, Little SJ, Everitt BJ. Differential involvement of NMDA, AMPA/kainate, and dopamine receptors in the nucleus accumbens core in the acquisition and performance of pavlovian approach behavior. J Neurosci. 2001; 21(23):9471–9477. [PubMed: 11717381]
13. Gradinaru V, Zhang F, Ramakrishnan C, Mattis J, Prakash R, Diester I, Goshen I, Thompson KR, Deisseroth K. Molecular and cellular approaches for diversifying and extending optogenetics. Cell. 2010; 141(1):154–165. [PubMed: 20303157]
14. Wright CI, Groenewegen HJ. Patterns of convergence and segregation in the medial nucleus accumbens of the rat: relationships of prefrontal cortical, midline thalamic, and basal amygdaloid afferents. J Comp Neurol. 1995; 361(3):383–403. [PubMed: 8550887]
15. McFarland K, Lapish CC, Kalivas PW. Prefrontal Glutamate release into the core of the nucleus accumbens mediates cocaine induced reinstatement of drug-seeking behavior. J Neurosci. 2003; 23(8):3531–3537. [PubMed: 12716962]
16. Kalivas PW, Volkow N, Seamans J. Unmanageable Motivation in Addiction: A Pathology in Prefrontal-Accumbens Glutamate Transmission. Neuron. 2005; 45(5):647–650. [PubMed: 15748840]
17. Schultz W. Predictive reward signal of dopamine neurons. J Neurophys. 1998; 80:1–27.
18. Bromberg-Martin ES, Hikosaka O. Midbrain dopamine neurons signal preference for advance information about upcoming rewards. Neuron. 2009; 63(1):119–126. [PubMed: 19607797]
19. Floresco SB, Yang CR, Phillips AG, Blaha CD. Basolateral amygdala stimulation evokes glutamate receptor-dependent dopamine efflux in the nucleus accumbens of the anaesthetized rat. The European Journal of Neuroscience. 1998; 10(4):1241–1251. [PubMed: 9749778]
20. Jones JL, Day JJ, Aragona BJ, Wheeler RA, Wightman RM, Carelli RM. Basolateral amygdala modulates terminal dopamine release in the nucleus accumbens and conditioned responding. Biol Psychiatry. 2010; 67(8):737–744. [PubMed: 20044074]
21. Aravanis AM, et al. An optical neural interface: *in vivo* control of rodent motor cortex with integrated fiberoptic and optogenetic technology. J Neural Eng. 2007; 4:S143–156. [PubMed: 17873414]

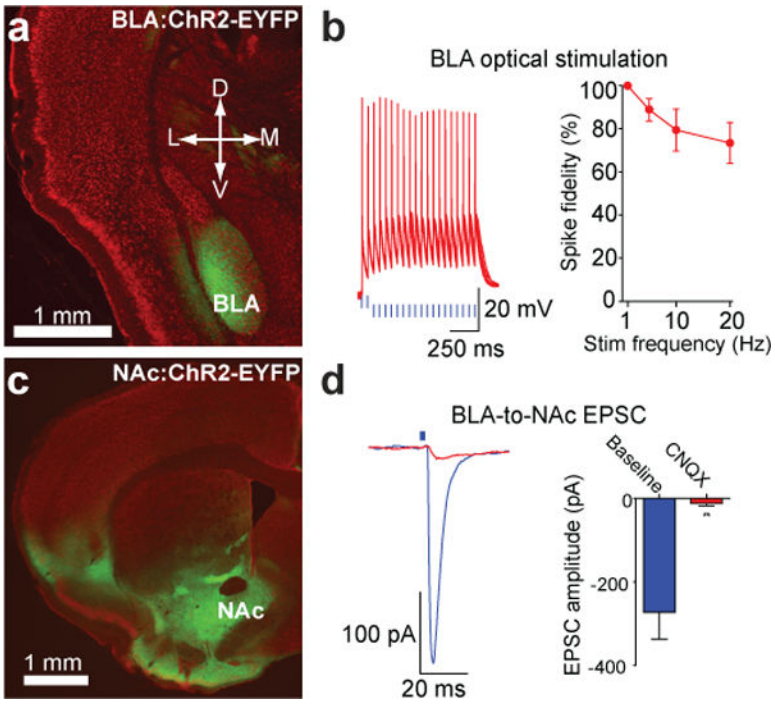

Figure 1. Expression of ChR2-EYFP in BLA neurons and fibers projecting to the NAc

a, Red fluorescent Nissl stained coronal brain slice showing expression of ChR2-EYFP (green) following virus injection in the BLA. **b**, Example traces and average data of current-clamped ChR2-expressing BLA neurons action potentials in response to 5-ms light pulses(*n* = 7 cells, *P* = 0.015). **c**, Expression of ChR2-EYFP in the NAc following virus injection in the BLA. **d**, EPSCs recorded from NAc neurons following optical stimulation of BLA-to-NAc fibers before and after bath application of CNQX (*P* = 0.007; *n* = 4 cells). All error bars for all figures correspond to the S.E.M.

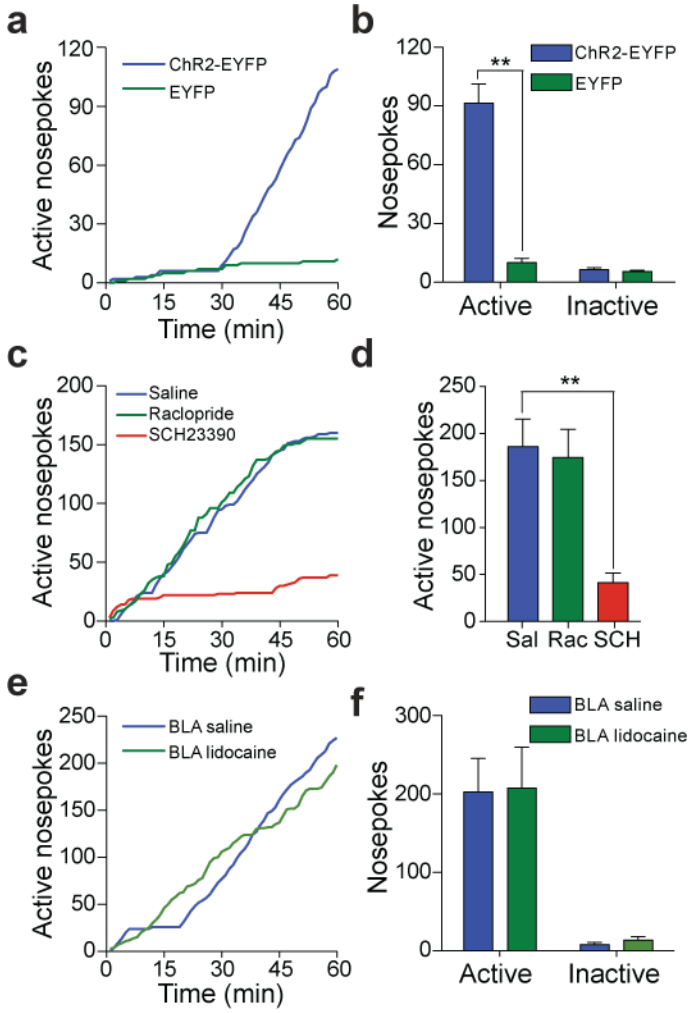

Figure 2. *In vivo* optical activation of BLA-to-NAc fibers promotes self-stimulation

a, Example cumulative activity graphs from the first behavioral session of active nosepokes made to obtain optical stimulation of BLA-to-NAc fibers in a ChR2-EYFP-expressing and a control mouse. **b**, Average nosepokes during the first optical self-stimulation session. (n = 12 ChR2-EYFP mice; n = 10 EYFP mice; $P < 0.0001$). **c**, Example cumulative activity graphs of nosepokes for optical stimulation following unilateral intra-NAc microinjections. **d**, Average nosepokes following intra-NAc microinjections (n = 19 saline; n = 11 SCH23390; n = 20 Raclopride, $P = 0.0016$). **e**, Example cumulative activity graphs of active nosepokes made for optical stimulation in mice that received intra-BLA vehicle or lidocaine. **f**, Average nosepokes following intra-BLA vehicle or lidocaine (n = 6 intra-BLA saline group; n = 6 intra-BLA lidocaine, $P = 0.88$.)

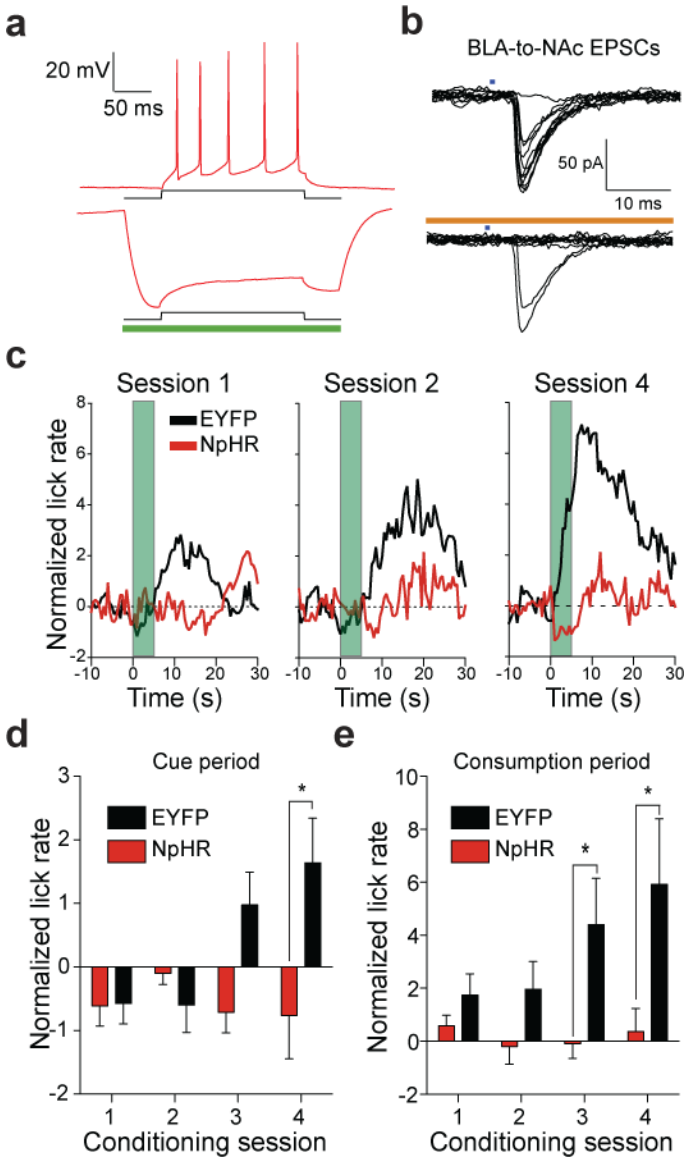

Figure 3. *In vivo* optical inactivation of BLA-to-NAc fibers reduces behavioral responding for sucrose

a, +100 pA current injection for 200 ms into NpHR expressing neurons in the BLA resulted in reliable spiking of BLA neurons (6.6 ± 0.9 spikes). In all neurons, NpHR-mediated hyperpolarization completely blocked spikes due to the current injection ($P = 0.02$, n = 3). **b**, ChR2 (473 nm) evoked EPSCs at BLA-to-NAc synapses are reduced when NpHR is activated (593.5 nm) in the same pathway. **c**, Average normalized lick rates (z-score) time-locked to cue onset (t = 0 – 5 s, green bar) and sucrose delivery (t = 5 s) for NpHR-and EYFP-expressing mice. BLA-to-NAc fibers were transiently inactivated (from t = −0.2 – 5.2 s) in NpHR-expressing mice on each trial of each conditioning session. **d,e**, Data from **c** broken into time bins corresponding to the cue period (t = 0 – 5 s) or the sucrose consumption period (t = 5 – 15 s). Lick rates were significantly attenuated during the cue period (**e**) in mice receiving BLA-to-NAc inhibition ($P = 0.013$ for treatment, n = 7 mice per

group). Lick rates were also significantly reduced during the sucrose consumption period (**f**) ($P = 0.001$ for treatment, n = 7 mice per group).

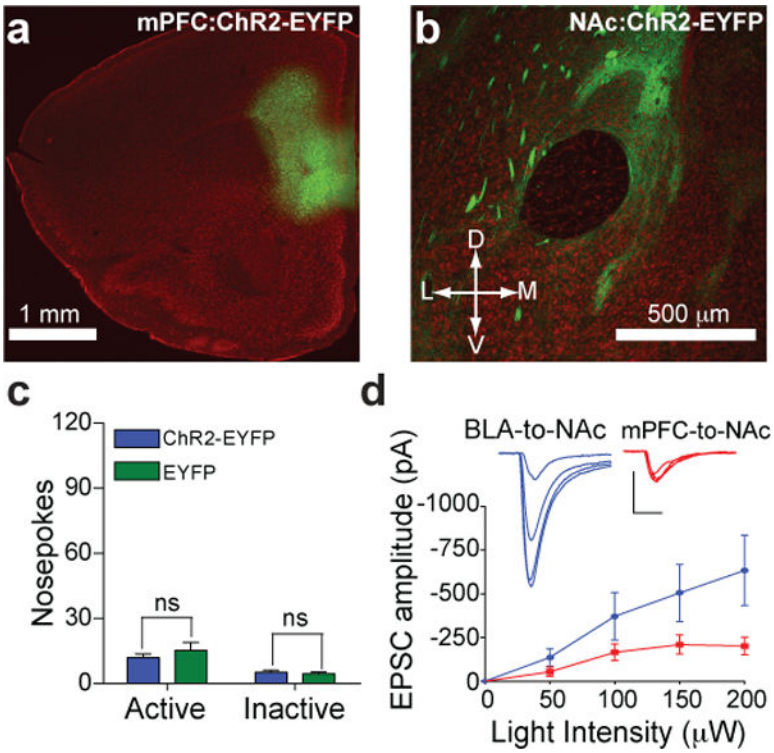

Figure 4. ***In vivo*** **optical activation of mPFC-to-NAc fibers does not promote self-stimulation**

a, Expression of ChR2-EYFP (green) following virus injection in the mPFC. **b**, Expression of ChR2-EYFP in fibers originating in the mPFC and innervating the NAc. **c**, Average nosepokes made by mice expressing ChR2-EYFP in mPFC-to-NAc fibers and controls (ChR2-EYFP n = 12 mice; EYFP n = 10 mice; P = 0.333). **d**, EPSCs recorded from NAc neurons evoked by either mPFC or BLA-to-NAc optical stimulation at increasing light intensities (n = 7 cells per group, effect for stimulated input: P = 0.003).